Title	A Neutron Detector with Submicron Spatial Resolution using Fine-grained Nuclear Emulsion
Author(s)	Naganawa, N.; Awano, S.; Hino, M.; Hirose, M.; Hirota, K.; Kawahara, H.; Kitaguchi, M.; Mishima, K.; Nagae, T.; Shimizu, H.M.; Tasaki, S.; Umemoto, A.
Citation	Physics Procedia (2017), 88: 224-230
Issue Date	2017
URL	http://hdl.handle.net/2433/234983
Right	© 2017 The Authors. Published by Elsevier B.V. This is an open access article under the CC BY-NC-ND license (http://creativecommons.org/licenses/by-nc-nd/4.0/).
Type	Journal Article
Textversion	publisher

Available online at www.sciencedirect.com

ScienceDirect

Physics Procedia 88 (2017) 224 – 230

Physics Procedia

8th International Topical Meeting on Neutron Radiography, Beijing, China, 4-8 September 2016

A neutron detector with submicron spatial resolution using fine-grained nuclear emulsion

N. Naganawa[a] *, S. Awano[b], M. Hino[c], M. Hirose[d], K. Hirota[b], H. Kawahara[b], M. Kitaguchi[b], K. Mishima[e], T. Nagae[d], H. M. Shimizu[b], S. Tasaki[f], A. Umemoto[b].

[a]*Institute of Materials and Systems for Sustainability, Nagoya University, Chikusa, Nagoya, 464-8602, Japan*
[b]*Department of Physics, Nagoya University, Chikusa, Nagoya, 464-8602, Japan*
[c]*Research Reactor Institute, Kyoto University, Kumatori, Osaka 590-0494, Japan*
[d]*Department of Physics, Kyoto University, Kyoto 606-8502, Japan*
[e]*High Energy Accelerator Research Organization, Tokai, Ibaraki 319-1106, Japan*
[f]*Department of Nuclear Engineering, Kyoto University, Kyoto 615-8540, Japan*

Abstract

We developed a neutron detector with submicron spatial resolution by incorporating ^{6}Li into a fine-grained nuclear emulsion. Upon exposure to thermal neutrons, tracks from neutron capture events were observed. The detector spatial resolution was estimated from their grain density. Detection efficiency was measured using the detector response to cold neutrons.

Peer-review under responsibility of the organizing committee of ITMNR-8

Keywords: neutron ; detector ; high spatial resolution ; submicron ; nuclear emulsion

1. Introduction

The importance of neutron detectors with high spatial resolution in neutron imaging is increasing. These days, development of imaging systems with thin scintillators including Gd compounds and cameras as CCD or sCMOS with magnification optics are improving resolving power steadily (Trtik and Lehman (2016), Hussey et al. (2016),

* Corresponding author. Tel.: +81-52-789-3532; fax: +81-52-789-2864.
E-mail address: naganawa@flab.phys.nagoya-u.ac.jp

Peer-review under responsibility of the organizing committee of ITMNR-8
doi:10.1016/j.phpro.2017.06.031

and Kardjilov et al. (2016)). The first two works reached that of about 5 μm. In other methods, MCPs doped with ^{10}B or Gd with fast readout electronics are being developed for neutron detection with high spatial resolution, high counting rate, and high detection efficiencies (Tremsin (2012) and Wang (2015)).The former work reached the spatial resolution of sub 15 μm. We have been developing detectors with submicron spatial resolution. These detectors are fabricated by incorporating 6Li, an isotope with a large neutron absorption cross section, into a fine-grained nuclear emulsion. A fine-grained emulsion is a three-dimensional tracking detector with a high spatial resolution. Using this technique, the resolution of imaging can be improved by more than an order of magnitude. Our detector requires a development process after exposure, and therefore it does not suit radiographies that require real-time information. It integrates information through an exposure time as an imaging plate, but works with much higher resolution. Unlike pixel detectors, it can provide higher spatial resolution without the constraint of pixel size. Another characteristic of our detector is that it is strong to gamma ray background, because fine-grained nuclear emulsion doesn't detect electron tracks from the conversion of gamma ray. This is an advantage comparing to the systems with scintillators using Gd compounds. Such an emulsion detector can also be used for fundamental physics experiments that require the measurement of the neutron interference pattern, such as searches for displacement from the inverse square law in the position distribution of quantized states of ultra-cold neutrons under the earth's gravitational field (Nesvizhevsky et al. (2002), Abele et al. (2009), Ichikawa et al. (2014)).

2. A neutron detector using nuclear emulsion

2.1. Nuclear emulsion

A nuclear emulsion detector is a three-dimensional tracking detector that detects charged particles with a submicron spatial resolution. It is a kind of photographic film, made using a substrate of plastic or glass coated with nuclear emulsion gel containing silver halide crystals dispersed in gelatin. The typical diameter of these crystals is about 200 nm. Their small size is the reason for the high spatial resolution. When a charged particle passes through the emulsion layer and the crystals in it, clusters of silver atoms are formed inside the crystals. These clusters are referred to as latent images. During emulsion development, these clusters turn into silver grains with diameters several times larger than the crystals, and they can then be identified using an optical microscope. In this way, the particle track can be made visible.

In 2010, a nuclear emulsion with higher resolution was developed at Nagoya University. It is a fine-grained nuclear emulsion with a crystal size of 40 nm, and it was developed for the detection of recoil tracks of WIMPs (Weakly Interacting Massive Particles) used in the search for dark matter (Naka and Natsume (2007), Naka et al. (2013)).

2.2 Application of nuclear emulsion to neutron detection with high spatial resolution

2.2.1 Nuclear emulsion gel

The fine-grained nuclear emulsion gel is applied to our high spatial resolution neutron detector, for two reasons. The first reason is that it gives a high spatial resolution owing to the small size of silver halide crystals. The second is that it has a low sensitivity to the gamma ray background. When used without sensitization, electron tracks from the conversion of gamma rays are not detected.

2.2.2 Detection principle

The nuclear emulsion is used as a neutron detector by incorporating nuclides with large neutron absorption cross sections into the emulsion. These nuclides emit charged particles after absorption of a neutron. In the case of ^{6}Li, neutrons will be absorbed by ^{6}Li and converted into charged particles by the process shown in equation (1) below.

$$n + {}^{6}\mathrm{Li} \rightarrow \alpha\ (2.05\ \mathrm{MeV}) + t\ (2.73\ \mathrm{MeV}) \quad (1)$$

When a neutron, n, is absorbed by ^{6}Li, an alpha particle, α, and a triton, t, with kinetic energies of 2.05 MeV and 2.73 MeV, respectively, are emitted. After the development of the emulsion, a back-to-back topology formed by their tracks, as shown in Fig.1, can be observed under an optical microscope.

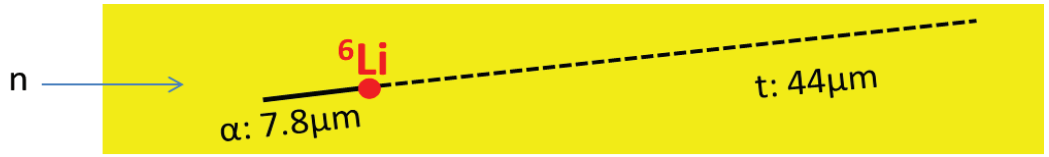

Fig. 1. After the absorption of neutron by ^{6}Li incorporated in a nuclear emulsion of silver halide crystals dispersed in gelatin, an alpha particle and a triton are emitted. A back-to-back topology is formed by their tracks. The expected length of tracks of the alpha particle and the triton are 7.8 μm and 44 μm respectively. These expected lengths were calculated using SRIM.

In a previous work (Taylor and Goldhaber (1935)), they incorporated ^{6}Li in nuclear emulsion and observed tracks of charged particles emitted after absorption of thermal neutrons. In our study, we incorporated ^{6}Li into a fine-grained nuclear emulsion. Owing to the resulting high spatial resolution of the detector, the individual grains within the emitted particle tracks were visible. This enabled measurement of the grain density (GD) of tracks. GD is defined as the number density of aligned silver grains along the particle tracks. From the measured GD and the track length, the particles which created those tracks were identified. As a result, the starting point of the tracks of alpha particles and tritons, i.e. the absorption points of the neutrons, were defined.

In this study we incorporated up to 1.2×10^{-3} mol/cm^3 of ^{6}Li into the nuclear emulsion, by incorporating $LiNO_3$ of up to 1.6×10^{-2} mol/cm^3. In this case, the track lengths of the alpha particle and the triton were calculated to be 7.7 μm and 44 μm respectively, using the Stopping and Range of Ions in Matter software (SRIM).

2.3 Fabrication of the detector

2.3.1 Incorporation of ^{6}Li into the nuclear emulsion gel

The fine-grained nuclear emulsion gel is melted at the temperature of 40 degrees centigrade. The liquid is stirred, and an aqueous solution of $LiNO_3$ is added by a micropipette. A final density of $LiNO_3$ in the dried emulsion gel was 1.6×10^{-2} mol/cm^3, corresponding to that of 1.2×10^{-3} mol/cm^3 of ^{6}Li in it. This amount is close to the maximum that can be added. If any more is added, the gel will not dry well, and the salt of $LiNO_3$ will be deposited on the surface of emulsion layer, reducing the detector effectiveness.

2.3.2 Coating

For the experiment described in section 3.1, a small amount of the liquid emulsion gel with the incorporated $LiNO_3$ was deposited on a 1 mm-thick glass plate using a micropipette, and spread using the pipette tip. For the experiment described in section 3.2, the glass plate was coated by dip coating. After coating, the glass plates were air dried in the room air. After drying, the thickness of the emulsion layer was 27 μm.

2.3.3 Packing of the detector

The nuclear emulsion is photosensitive. In order to protect our detector from light, we packed it in a light-tight package before use. The package is made of a foil consisting of nylon (15 μm), polyethylene (13 μm), aluminum (7 μm), polyethylene (13 μm), and black polyethylene (80 μm). The thickness of each material is written in brackets.

3. Neutron detection

3.1 Tracks and spatial resolution

To confirm the detection principle, a fabricated sample was exposed to thermal neutrons using the CN-3 beam line of a reactor at Kyoto University Research Reactor Institute. After the development of the emulsion film, absorption events were observed under an optical microscope with an epi-illumination system. A microscopic image of one of the observed events is shown in Fig. 2. The tracks of an alpha particle and a triton that emerged from an absorption point forming back-to-back topology can be clearly observed. Those tracks were identified by GD. From measurements on several absorption events, the first half sections of the alpha particles' tracks from the absorption point had an average GD of 1.4±0.4 grains/μm. Those of the tritons had that of 0.37±0.08 grains/μm. dE/dx of those particles were calculated by SRIM 2008. Their Bragg curves drawn from the result is shown in Fig. 3. The average dE/dx for the first half sections of their tracks were 9.04×10^2 MeV/(g/cm^2) and 1.61×10^2 MeV/(g/cm^2) for alpha particles and tritons, respectively. The difference between the ratio of the GD and the dE/dx was not significant.

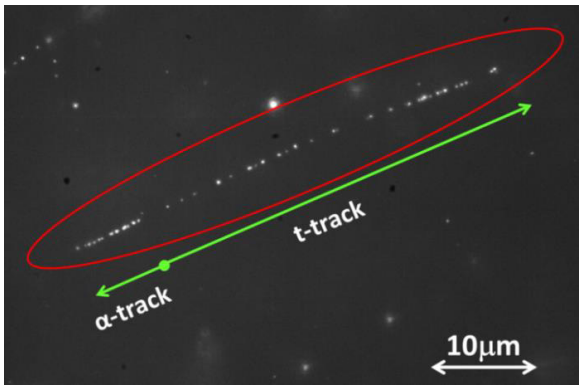

Fig. 2. An example of a neutron absorption event by ^{6}Li observed under an optical microscope with an epi-illumination system (circled in red). A pair of tracks of an alpha particle and a triton (green arrows) in back-to-back topology was identified.

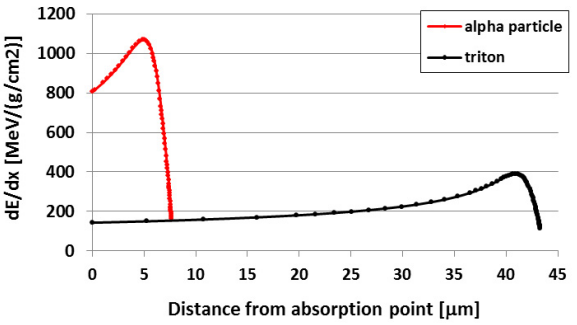

Fig. 3. Bragg curves of an alpha particle and a triton emitted from a neutron absorption point. dE/dx were calculated by SRIM 2008.

Next, we estimated the spatial resolution of the detection of neutron absorption points, i.e. the precision of determining their positions. In our emulsion detector, grains forming tracks exist discretely. Therefore, a gap between the first grain of an alpha track and an absorption point exists. The gap determines the precision of the detector. When dE/dx does not change rapidly, we can assume that positions of grains of a track follow Poisson distribution (O'Ceallaigh (1954)). The probability (P) of the absorption point existing between 0 and x μm upstream from the first grain of the alpha track is described using the average GD, $\langle n \rangle$ grains/μm as

$$P = 1 - \exp(-\langle n \rangle x) . \quad (2)$$

An average GD of the first half section of alpha tracks from 10 absorption events was 1.7±0.3 grains/μm. From the Bragg curve in Fig. 3., the average dE/dx in the section differs only 10% from the dE/dx at the absorption point. Therefore, we can use the average GD value and the assumption of Poisson distribution in this calculation. By substituting this value as <n> in formula (2), the absorption point exists in the interval between 0 and 0.67 μm upstream from the first grain of the alpha track with the probability of 68 %. We determine the center of the interval as the candidate position of absorption point. The real absorption point exists between 0.34 μm upstream and downstream from the center with the same probability. Thus, the precision, i.e. the spatial resolution was estimated to be 0.34 μm. By raising the GD by improvement of the development method, it will be possible to realize a higher resolution.

3.2 Detection efficiency

3.2.1 Exposure

The detection efficiency was measured by exposing an emulsion detector to a pulsed cold neutron beam with a wavelength range of 0.2 to 1.0 nm at the Low Divergence Beam Branch of BL05 in MLF/J-PARC (Mishima et al. (2009), Mishima (2015)). The repetition rate of the neutron pulse is 25 Hz. The experimental set up during the exposure is shown in Fig. 4. A pinhole with diameter of 1.1 mm made using a 1 mm-thick Cd plate was set upstream of the fabricated emulsion detector. Downstream from the detector, the intensity of the neutron beam was measured by a 25.4 mm diameter 0.97 MPa-^{3}He proportional counter, RS-P4-0812-223, with a 0.5 mm-thick stainless steel wall. The wavelength distribution of neutrons that passed through the pinhole was as shown in Fig. 5. This distribution was derived from time of flight information taken by the ^{3}He counter, without setting the emulsion detector. The sample was exposed to $(4.2\pm0.4) \times 10^5$ neutrons in total, which passed though the pinhole. The uncertainty of the neutron intensity is 10 %, mainly due to a conservative estimate of the uncertainty of the detection efficiency of the ^{3}He detector.

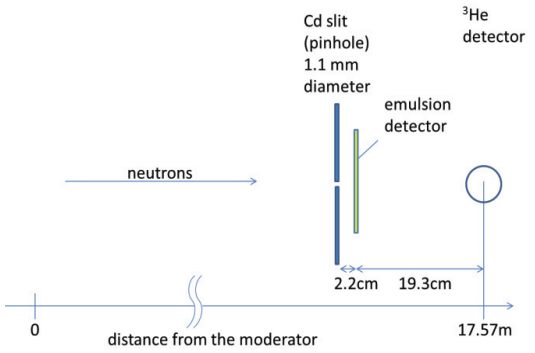

Fig. 4. The experimental set up during the exposure. A 1.1 mm pinhole (Cd slit) was set 2.2 cm upstream from the emulsion detector. A ^{3}He detector was placed 19.3 cm downstream from the emulsion detector.

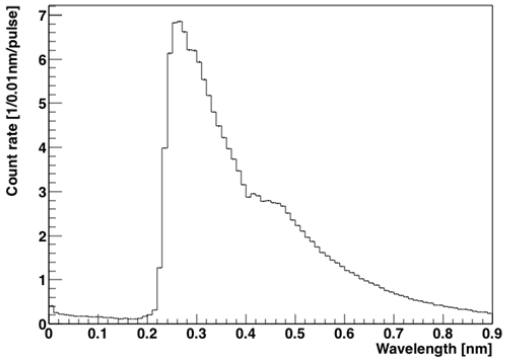

Fig. 5. The wavelength distribution measured through the pinhole by the downstream ^{3}He detector..

3.2.2 Analysis

The emulsion was developed after the exposure. In order to calculate detection efficiency, it was necessary to count the number of absorption events in the neutron-exposed area. This counting was done manually, under an optical microscope with an epi-illumination system. To minimize the time for counting, only defined sample areas were investigated. These areas are shown in Fig. 6. There were 25 sample areas on the emulsion. Of these, 21 were within the 1.1 mm diameter corresponding to the pinhole area. The field of view of the microscope was (110 μm × 110 μm). The entire 27 μm thickness of the emulsion layer was investigated. For the calculation of the detection efficiency, the total number of events in the 21 regions was used. The total area of the 21 regions was 2.5×10^{-3} cm^2.

In order to accurately determine the absorption point by the difference in the GD of the alpha and triton tracks, we only accept events with alpha and triton tracks that have at least three grains in the emulsion layer. This requirement reduces the efficiency of counting neutrons to (81±9) % of the absorbed neutron. This value of efficiency reduction was calculated numerically from geometry.

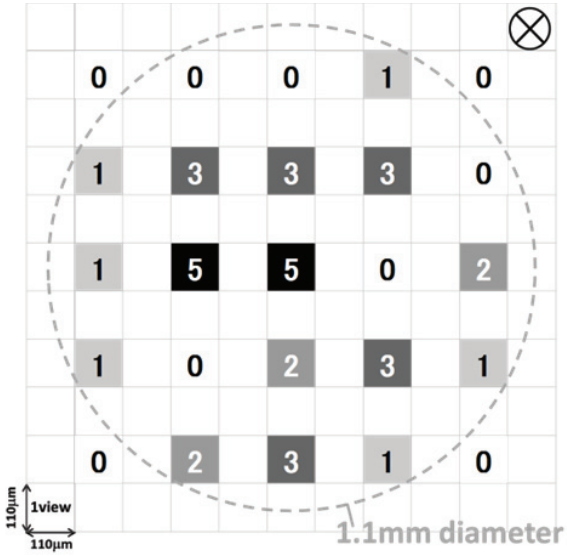

Fig. 6. Schematic representation of areas in which absorption events were counted. The dashed circle represents the 1.1 mm diameter area of the upstream Cd pinhole. Each square corresponds to the field of view of the microscope (110 μm × 110 μm). The number inside each box corresponds to the number of absorption events found within the region. Regions outside the pinhole area were not investigated. The total number of events in the 21 regions inside the dashed circle was used for the measurement of detection efficiency.

3.2.3 Results

A total of 37 absorption events were detected in the 21 regions. The total number of neutrons this area was exposed to was $(1.1\pm0.1) \times 10^5$. By considering the wavelength distribution in Fig. 5 and knowing that the absorption cross section is proportional to the inverse of the velocity, the expected number of absorption events in the investigated regions was calculated to be (44±5) events. Including the requirement of a minimum of three grains in the emulsion layer per track discussed in the previous section, (81±9) % of them, or (36±6) events were expected. The number of detected events (37) was consistent with this calculation.

The detection efficiency calculated from this result is $(3.3\pm0.6) \times 10^{-4}$ for the cold neutrons in this experiment. Extrapolating this result, the detection efficiency for thermal neutrons with a velocity of 2200 m/s is $(1.5\pm0.5) \times 10^{-4}$.

4. Conclusion and outlook

We developed a neutron detector with submicron spatial resolution by incorporating ^{6}Li into a fine-grained nuclear emulsion. Events of neutron absorption by ^{6}Li were successfully observed from the exposure to thermal neutrons. From the grain density (GD) of the observed alpha tracks, the spatial resolution of detection of the absorption point was estimated to be 0.34 μm. Further improvement of the resolution is possible with improvement of a development method for the emulsion that increases the GD.

The detection efficiency was measured by a test exposure to cold neutrons. The efficiency was measured as $(3.3\pm0.6) \times 10^{-4}$, which was consistent with the expectation. By extrapolation of this result, the detection efficiency of thermal neutrons with velocity of 2200 m/s was calculated to be $(1.5\pm0.5) \times 10^{-4}$.

With this detector, it is possible to increase the spatial resolution of neutron radiography by more than an order of magnitude, if with an exposure using well collimated neutrons. The detector can also be used for fundamental physics experiments that require the measurement of neutron interference patterns. Future work will study the uniformity of the detection efficiency and distortion of the detector.

Acknowledgments

We acknowledge Dr. Y. Seki for sharing his beam time and helping our exposure at KURRI. The efficiency measurement was approved by the Neutron Science Proposal Review Committee of J-PARC/MLF (Proposal No. 2014B0270 and 2015A0242) and supported by the Inter-University Research Program on Neutron Scattering of IMSS, KEK. This work was supported by JSPS KAKENHI Grant Number JP26800132.

References

Abele, H. et al., Nuclear Physics A 827 (2009) 593c–595c.
Hussey, D. S., et al., ECS Transactions. 75 (14), (2016) 245–250.
Ichikawa, G. et al., Phys. Rev. Lett. 112, (2014) 071101.
Kardjilov, N., et al., J. Appl. Cryst. 49, (2016) 195–202.
Mishima, K. et al., Nuclear Instruments and Methods in Physics Research A 600, (2009) 342–345.
Mishima, K., Neutron network news (Hamon) 25 (2), (2015) 156–160.
Naka, T., Natsume, M., Nuclear Instruments and Methods in Physics Research A 581, (2007) 761–764.
Naka, T. et al., Nuclear Instruments and Methods in Physics Research A 718, (2013) 519–521.
Nesvizhevsky, V. V. et al., Natrue, 415, (2002).
O'Ceallaigh, C., Il Nuovo Cimento 2, (1954) 412–415.
Taylor, H. J., Goldhaber, M, Nature, 135 (3409), (1935) 341.
Tremsin, A. S., Newtron News 23 (4), (2012) 35–38
Trtik, P., Lehman, E. H., Journal of physics: Conference Series 746, (2016) 012004.
Wang, Y., Nuclear Instruments and Methods in Physics Research A 784, (2015) 226–231.